

# A Chiral Bis(oxazoline) Phosphine with a Rigid Backbone: Ligand Synthesis and Characterization of Products Obtained in Highly Diastereoselective Reactions with a Rhodium(I) Complex and a Tetrahedral “RhRu<sub>3</sub>” Cluster

Igor O. Koshevoy and Sergey P. Tunik\*

Department of Chemistry, St. Petersburg University, Universitetskii pr., 26,  
St. Petersburg 198504, Russian Federation

Anthony J. Poë and Alan Lough

Lash Miller Chemical Laboratories, University of Toronto, 80 St. George Street, Toronto,  
Ontario, Canada M5S 3H6

Jouni Pursiainen

Department of Chemistry, University of Oulu, P.O. Box 3000, FIN-90014 Oulu, Finland

Päivi Pirilä

Biocenter and Department of Biochemistry, University of Oulu, P.O. Box 3000,  
FIN-90014 Oulu, Finland

Received March 2, 2004

A novel bis(oxazoline)–thienylphosphine ligand (**3**, abbreviated as (*S,S*)-BOTPHOS) has been synthesized in an enantiomerically pure *S,S* state and spectroscopically characterized. The reaction of **3** with Rh<sub>2</sub>(CO)<sub>4</sub>Cl<sub>2</sub> in a dichloromethane solution affords the mononuclear Rh(Cl)<sub>2</sub>(CH<sub>2</sub>Cl)(κ<sup>3</sup>-(*S,S*)-BOTPHOS) octahedral complex (**4**), containing BOTPHOS coordinated to the Rh(III) center in a *mer* mode through the phosphorus atom and the two nitrogens of the oxazoline fragments. The coordination sphere of this complex displays an unusual rigidity, which is determined by intramolecular hydrogen bonding between the chlorides and protons of the organic ligands. Treatment of the CpRhRu<sub>3</sub>(H)<sub>2</sub>(CO)<sub>10</sub> cluster with a slight excess of (*S,S*)-BOTPHOS results in the substitution of two carbonyls at a ruthenium atom and chelate coordination of the ligand through the phosphorus and a nitrogen atom of an oxazoline ring to give CpRhRu<sub>3</sub>(H)<sub>2</sub>(CO)<sub>8</sub>(κ<sup>2</sup>-(*S,S*)-BOTPHOS) (**5**). The bidentate coordination mode of BOTPHOS makes the phosphorus atom of this ligand chiral and simultaneously differentiates the ruthenium vertexes in the tetrahedral RhRu<sub>3</sub> cluster. This differentiation generates an asymmetry in the cluster framework and introduces a fourth chiral center in the cluster molecule. A specific feature of this reaction consists of the quantitative diastereoselection induced by the chirality of the BOTPHOS oxazoline fragments. This induction produces only *S* configurations in both of the new chiral elements generated in the cluster molecule. Molecular structures of the complexes obtained have been established by X-ray crystallography and have been confirmed by the NMR spectroscopic study of these compounds in solution. CD spectroscopic measurements of **3**–**5** indicate that these compounds have been obtained in their enantiopure state.

## Introduction

In the fast-growing field of asymmetric catalysis the ability to tune a catalyst's properties to produce an optimum reactivity pattern plays a central role. This is usually accomplished by modifying the chiral ligands' characteristics through changes to the number and nature of the ligands' donor centers themselves, as well as by tuning the properties of any chiral

auxiliaries present. In this context, the homo- and heterotopic chiral ligands based on asymmetric oxazoline moieties provide unique opportunities.<sup>1,2</sup> Multidentate (P,N; S,N; N,N,N; N,P,N) coordination of the ligands to a metal center makes it possible to support the chiral information on a rigid “platform”. On the other hand, the modular structure of the multidentate ligands allows for extensive variations in their backbones and

\* To whom correspondence should be addressed. E-mail: stunik@chem.spbu.ru.

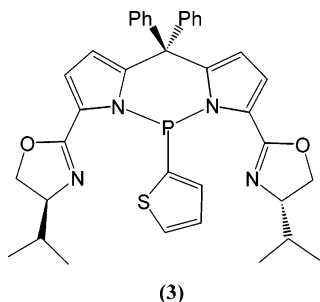
(1) Helmchen, G.; Pfaltz, A. *Acc. Chem. Res.* **2000**, *33*, 336.

(2) Braunstein, P.; Naud, F. *Angew. Chem., Int. Ed.* **2001**, *40*, 680.

so enables detailed control of the ligands' properties. Additionally, the general approach to the synthesis of asymmetric oxazoline fragments provides the opportunity to fine-tune the chiral pocket by variations in the nature and steric characteristics of the oxazoline substituents. It is worth noting that bonding of the oxazoline ligands to a metal usually occurs via the nitrogen atoms. This brings the chiral center of the oxazoline ring into the immediate vicinity of the metal atom in a way that evidently increases chiral induction of the corresponding catalysts. Another important feature of this class of ligands is the ease with which they can be prepared in enantiopure states using readily available and inexpensive natural precursors such as  $\alpha$ -amino acids and/or  $\alpha$ -amino alcohols.

Since the first reported preparation of oxazolines,<sup>3</sup> aimed at application in asymmetric synthesis, a wide variety of those ligands and corresponding complexes have been synthesized and used in asymmetric catalysis.<sup>1,2</sup> Due to the stability of their complexes under catalytic conditions, and the rigidity of the ligand conformation in the coordination sphere of the catalysts, particular attention has also been paid to multidentate ligands that contain donor functionalities other than oxazoline nitrogens. Polydentate ligands containing additional aromatic nitrogen (NNN)<sup>4</sup> and phosphorus-(III) functionalities (PN,<sup>1,5</sup> NPN<sup>6,7</sup>) have been synthesized and their mononuclear complexes successfully applied in various catalytic reactions, including hydrogenation of unfunctionalized olefins,<sup>8,9</sup> hydrosilylation of ketones,<sup>4</sup> cyclopropanation of olefins,<sup>10</sup> and reduction of imines.<sup>9</sup>

However, it has to be noted that the number of oxazoline-based tridentate chiral ligands is still quite limited. The tridentate coordination of these ligands makes their backbone exceptionally rigid in a way that gives rise to high stereoselection of the chiral auxiliaries in stoichiometric and catalytic reactions. Development of their synthesis and coordination chemistry is therefore very important in creating a broad background for preparation of novel catalysts and fine-tuning their catalytic properties. In the present paper we describe the efficient, simple and inexpensive synthesis of the new type of chiral bis(oxazoline)phosphino ligand



and the study of its coordination to a mononuclear rhodium center and to a tetranuclear "RhRu<sub>3</sub>" cluster.

### Experimental Section

**General Comments.** P(2-thienyl)Cl<sub>2</sub>,<sup>11</sup> diphenyldipyrromethane,<sup>12</sup> L-valinol,<sup>13</sup> Rh<sub>2</sub>(CO)<sub>4</sub>Cl<sub>2</sub>,<sup>14</sup> and (C<sub>5</sub>H<sub>5</sub>)RhRu<sub>3</sub>(H)<sub>2</sub>-

(CO)<sub>10</sub><sup>15</sup> were synthesized according to published procedures. Reagent grade solvents—acetonitrile, chlorobenzene, chloroform, dichloromethane, diethyl ether, dimethyl formamide (DMF), ethanol, hexane, octane, and toluene—were used as received. Tetrahydrofuran was distilled over Na—benzophenone ketyl under a nitrogen atmosphere prior to use. Exact mass peaks (for compounds 1–5) were determined on a Micromass LCT instrument, using the ESI+ method. Circular dichroism (CD) spectra were recorded on a Jasco J-715 spectropolarimeter. The IR spectra were recorded on a Nicolet 550 Magna FTIR spectrometer. Microanalyses were carried out in the Analytical Laboratory of the University of Toronto. The <sup>1</sup>H, <sup>13</sup>C, and <sup>31</sup>P NMR spectra were recorded on Bruker DPX 200, Bruker DPX 300, Gemini 300, and Unity 500 spectrometers. The chemical shifts were referenced to residual solvent resonances for the <sup>1</sup>H and <sup>13</sup>C spectra and external 85% H<sub>3</sub>PO<sub>4</sub> in the <sup>31</sup>P spectra. The accuracy of the temperature measurements in variable-temperature NMR experiments was  $\pm 1.0$  °C.

**1,9-Dicyano-5,5-diphenyldipyrromethane (1).** Diphenyldipyrromethane (5.4 g, 18.1 mmol) was dissolved in DMF (100 cm<sup>3</sup>) and the solution diluted with acetonitrile (40 cm<sup>3</sup>). The solution was cooled to ca.  $-50$  °C, and chlorosulfonyl isocyanate (CSI; 9 g, 63.6 mmol, 3.5 equiv) in acetonitrile (40 cm<sup>3</sup>) was slowly added with stirring over a period of ca. 1.5 h. The reaction mixture was then warmed slowly to room temperature. The resulting orange-red transparent solution was stirred for an additional 1 h, concentrated to ca. 20 mL, and diluted with absolute ethanol (20 cm<sup>3</sup>) to give a dark solution. Water (ca. 90 mL) was carefully added to cause precipitation of a crude product, which was collected by filtration and washed with ethanol/H<sub>2</sub>O (1/1, v/v) mixture (3  $\times$  15 cm<sup>3</sup>). The residue was vacuum-dried to give a creamy powder (4.5 g, 71%), which was used in the further syntheses without additional purification. To determine spectroscopic characteristics of the product, it was recrystallized from CH<sub>2</sub>Cl<sub>2</sub>/hexane. ES MS (*m/z*): [M<sup>+</sup>] 348 (calcd 348). <sup>1</sup>H NMR (CDCl<sub>3</sub>;  $\delta$ ): 7.91 (br s, NH, 2H), 7.24, 7.08 (m, Ph, 10H), 6.72 (m, pyrrole, 2H), 6.15 (pseudo-quartet, pyrrole, 2H), 5.94 (m, pyrrole, 2H).

**4(S)-Isopropyl-2-[[5-[5-(4(S)-isopropyl-4,5-dihydro-1,3-oxazol-2-yl)-1H-pyrrol-2-yl](diphenyl)methyl]-1H-pyrrol-2-yl]-4,5-dihydro-1,3-oxazole (2).** ZnCl<sub>2</sub> (1.37 g, 10 mmol) was melted in vacuo and cooled under an atmosphere of argon for 20–25 min. A slurry of **1** (6.8 g, 19.5 mmol) and L-valinol (5.2 g, 50.5 mmol, 2.6 equiv) in chlorobenzene (60 cm<sup>3</sup>) was added, and the reaction mixture was refluxed for 24 h. The solvent was then removed in vacuo, the brown solid obtained was suspended in ethanol (100 cm<sup>3</sup>), and 55 cm<sup>3</sup> of water was carefully added with vigorous stirring. The resulting creamy precipitate was collected by filtration, washed with ethanol/water (1/1, v/v; 20 cm<sup>3</sup>), suspended in acetone (15 cm<sup>3</sup>), and

(4) Nishiyama, H.; Kondo, M.; Nakamura, T.; Itoh, K. *Organometallics* **1991**, *19*, 500.

(5) Tang, W.; Zhang, X. *J. Am. Chem. Soc.* **2003**, *103*, 3029.

(6) Braunstein, P.; Naud, F.; Pfaltz, A.; Rettig, S. *J. Organometallics* **2000**, *19*, 2676.

(7) Yamagishi, T.; Ohnuki, M.; Kiyooka, T.; Masui, D.; Sato, K.; Yamaguchi, M. *Tetrahedron: Asymmetry* **2003**, *14*, 3275.

(8) Pfaltz, A.; Blankenstein, J.; Hilgraf, R.; Hormann, E.; McIntire, S.; Menges, F.; Schonleber, M.; Smidt, S. P.; Wustenberg, B.; Zimmermann, N. *Adv. Synth. Catal.* **2003**, *345*, 33.

(9) Cozzi, P. G.; Menges, F.; Kaizer, S. *Synlett* **2003**, 833.

(10) Nishiyama, H.; Itoh, Y.; Sugavara, Y.; Matsumoto, H.; Aoki, K.; Itoh, K. *Bull. Chem. Soc. Jpn.* **1995**, *68*, 1247.

(11) Bentov, M.; David, L.; Bergmann, E. D. *J. Chem. Soc.* **1964**, 4750.

(12) Freckmann, D. M. M.; Dube, T.; Berube, C. D.; Gambarotta, S.; Yap, G. P. A. *Organometallics* **2002**, *21*, 1240.

(13) Abiko, A.; Masamune, S. *Tetrahedron Lett.* **1992**, *33*, 5517.

(14) Krafft, M. E.; Wilson, L. J.; Onan, K. D. *Organometallics* **1988**, *7*, 2528–2534.

(15) Lindsell, W. E.; Knobler, C. B.; Kaesz, H. D. *J. Organomet. Chem.* **1985**, *296*, 209.

(3) Meyers, A. I.; Knaus, G. *J. Am. Chem. Soc.* **1974**, *96*, 268.

diluted with Et<sub>2</sub>O (10 cm<sup>3</sup>). The brown solution was decanted, and the residue was successively washed with acetone/Et<sub>2</sub>O (1/3, v/v; 15 cm<sup>3</sup>) and Et<sub>2</sub>O/hexane (1/1, v/v; 15 cm<sup>3</sup>) and vacuum-dried to give 5.8 g (57%) of **2**. The product was pure enough to be used in the further stages of the synthesis without additional purification. To obtain its spectroscopic characteristics, it was recrystallized from CH<sub>2</sub>Cl<sub>2</sub>/hexane. MS ES (*m/z*): [M<sup>+</sup>] 520 (calcd 520). <sup>1</sup>H NMR (CDCl<sub>3</sub>; δ): 12.07 (br s, NH, 2H), 7.14 and 6.82 (m, Ph, 10H), 6.45 (m, pyrrole, 2H), 6.02 (m, pyrrole, 2H), 3.76 (m, CH<sub>2</sub> oxazoline, 4H), 2.61 (m, CH, oxazoline, 2H), 0.85 (m, *i*-Pr CH, 2H), 0.61 (m, *i*-Pr CH<sub>3</sub>, 6H), 0.50 (m, *i*-Pr CH<sub>3</sub>, 6H).

**4(S)-Isopropyl-2-[7-(4(S)-isopropyl-4,5-dihydro-1,3-oxazol-2-yl)-10,10-diphenyl-5-(2-thienyl)-10H-dipyrrolo[1,2-c:2,1-f[1,3,2]]diazaphosphinin-3-yl][4,5-dihydro-1,3-oxazole ((S,S)-BOTPHOS, **3**).** **2** (2.8 g, 5.4 mmol) and Et<sub>3</sub>N (4 cm<sup>3</sup>) were dissolved in THF (75 cm<sup>3</sup>) under nitrogen. The solution was cooled to ca. -50 °C, and a slight excess of dichloro(2-thienyl)phosphine (1.26 g, 6.8 mmol) was added by syringe. The mixture was stirred for 30 min, slowly warmed to room temperature, and stirred for an additional 2 h. The brownish yellow solution was filtered, and the precipitate was washed with THF (2 × 15 cm<sup>3</sup>) and then Et<sub>2</sub>O (2 × 10 cm<sup>3</sup>). All the washings were combined with the filtrate, and the solvents were removed in vacuo. The crude product was extracted from this residue with a few portions of Et<sub>2</sub>O (3 × 15 cm<sup>3</sup>). The solvent was removed under reduced pressure, and the final product was extracted with a few portions of warm hexane (7 × 15 cm<sup>3</sup>). Removal of hexane gave an amorphous, slightly yellowish solid, which was suspended in 10 cm<sup>3</sup> of hexane and heated gently to ca. 40–45 °C to give a white crystalline solid and a yellowish solution. The suspension was cooled to ca. -40 °C, the yellowish solution was filtered, and the white to slightly yellowish solid was dried in vacuo. The washings were left to stand in air at room temperature, and some additional white crystalline product precipitated. Total yield: 1.9 g (56%). MS ES (*m/z*): [M<sup>+</sup>] 632 (calcd 632.7). <sup>31</sup>P{<sup>1</sup>H} NMR (CDCl<sub>3</sub>; δ): 57.1 (s). <sup>1</sup>H NMR (CDCl<sub>3</sub>; δ): 7.21–6.66 (Ph and thienyl multiplets, 13H), 6.26 (t, pyrrole, 1H, *J*(H–H) = 4.2 Hz), 6.00 (m, pyrrole, 2H), 5.55 (d, pyrrol, 1H, *J*(H–H) = 3.5 Hz), 4.44 (m, oxazoline CH<sub>2</sub>, 1H), 4.29 (m, oxazoline CH<sub>2</sub>, 1H), 4.16 (m, oxazoline CH<sub>2</sub>, 2H), 3.91 (m, oxazoline CH, 2H), 1.73 (m, *i*-Pr CH, 1H), 1.48 (m, *i*-Pr CH, 1H), 1.04 (m, *i*-Pr CH<sub>3</sub>, 6H), 0.61 (m, *i*-Pr CH<sub>3</sub>, 6H). Anal. Calcd for C<sub>37</sub>H<sub>37</sub>N<sub>4</sub>O<sub>2</sub>PS: C, 70.23; H, 5.89; N, 8.85; S, 5.07. Found: C, 70.23; H, 6.06; N, 8.86; S, 5.70.

**RhCl<sub>2</sub>(CH<sub>2</sub>Cl)((S,S)-BOTPHOS) (**4**).** A 100 cm<sup>3</sup> Schlenk tube was charged with crystalline Rh<sub>2</sub>(CO)<sub>4</sub>Cl<sub>2</sub> (27 mg, 0.069 mmol) and a 2-fold excess of **3** (92 mg, 0.145 mmol), thoroughly evacuated, and filled with nitrogen. Degassed dichloromethane (20 cm<sup>3</sup>) was transferred into the vessel to give a bright orange solution. The reaction mixture was stirred under nitrogen for ca. 24 h until its color changed to yellow and the <sup>31</sup>P NMR spectrum showed consumption of the starting ligand and formation of only one phosphorus-containing product. The solvent was removed in vacuo, and the yellow powder was recrystallized at room temperature from the CH<sub>2</sub>Cl<sub>2</sub>/Et<sub>2</sub>O/hexane mixture to give yellow-orange crystals of **4** (86 mg, 72%). MS (*m/z*): [M<sup>+</sup>] 805 (calcd 805). <sup>31</sup>P{<sup>1</sup>H} NMR (CDCl<sub>3</sub>, 25 °C; δ): 94.4 (d, *J*(P–Rh) = 157.8 Hz). <sup>1</sup>H NMR (CDCl<sub>3</sub>, 25 °C; δ): 7.33 (dd, thienyl, 1H, *J*(H–H) = 5.0, 1.1 Hz), 7.27 (m, Ph, 1H), 7.22 (m, Ph, 2H), 7.18 (m, pyrrolyl, 1H), 7.04 (m, pyrrolyl, 1H), 7.00 (m, Ph, 1H), 6.95 (m, Ph, 2H), 6.91 (m, Ph, 1H), 6.90 (m, Ph, 1H), 6.82 (m, Ph, 1H), 6.80 (m, Ph, 1H), 6.41 (m, thienyl, 1H), 6.26 (ddd, thienyl, 1H, *J*(H–P) = 8.3 Hz, *J*(H–H) = 3.5, 1.1 Hz), 6.10 (m, pyrrolyl, 2H), 5.60 (m, oxazoline CH, 1H), 4.99 (dd, CH<sub>2</sub>Cl, 1H, *J*(H–H) = 5.9 Hz, *J*(H–Rh) = 3.2 Hz), 4.87 (dm, oxazoline CH, 1H, *J*(H–H) = 8.1 Hz), 4.59 (dd, oxazoline CH<sub>2</sub>, 1H, *J*(H–H) = 8.4, 2.3 Hz), 4.52 (m, oxazoline CH<sub>2</sub>, 2H), 4.40 (dd, oxazoline

CH<sub>2</sub>, 1H, *J*(H–H) = 10.0, 8.6 Hz), 4.02 (dd, CH<sub>2</sub>Cl, 1H, *J*(H–H) = 5.9 Hz, *J*(H–Rh) = 2.7 Hz), 3.28 (m, *i*-Pr CH, 1H), 3.21 (m, *i*-Pr CH, 1H), 0.96 (d, *i*-Pr CH<sub>3</sub>, 3H, *J*(H–H) = 7.1 Hz), 0.83 (d, *i*-Pr CH<sub>3</sub>, 3H, *J*(H–H) = 7.1 Hz), 0.78 (d, *i*-Pr CH<sub>3</sub>, 3H, *J*(H–H) = 7.1 Hz), 0.63 (d, *i*-Pr CH<sub>3</sub>, 3H, *J*(H–H) = 7.1 Hz). Anal. Calcd for C<sub>38</sub>H<sub>39</sub>N<sub>4</sub>O<sub>2</sub>PSCl<sub>3</sub>Rh: C, 53.32; H, 4.59; N, 6.54. Found: C, 53.49; H, 4.83; N, 6.51. Single crystals of **4** suitable for X-ray analysis were grown from a CH<sub>2</sub>Cl<sub>2</sub>/Et<sub>2</sub>O/hexane mixture at room temperature.

**(η<sup>5</sup>-C<sub>5</sub>H<sub>5</sub>)RhRu<sub>3</sub>(μ-H)<sub>2</sub>(CO)<sub>8</sub>(1,1-κ<sup>2</sup>-BOTPHOS) (**5**).** CpRhRu<sub>3</sub>(H)<sub>2</sub>(CO)<sub>10</sub> (140 mg, 0.19 mmol) and a slight excess of **3** (149 mg, 0.24 mmol) were dissolved in toluene (35 cm<sup>3</sup>). Nitrogen was continuously bubbled through the solution while the reaction mixture was stirred at room temperature for ca. 60 h, at which time a TLC spot test showed complete consumption of the starting cluster. By this time the solution had changed color from dark brown to dark red. The solvent was removed in vacuo to give an oily residue, which was dissolved in hexane (3 cm<sup>3</sup>), leaving some dark insoluble material. The solution was decanted, diluted with dichloromethane (2 cm<sup>3</sup>), and transferred onto a chromatographic column (silica 5–40 mesh, 2.5 × 10 cm). Elution with hexane/CH<sub>2</sub>Cl<sub>2</sub>/Et<sub>2</sub>O (5/2/0.2, v/v/v) gave a few unidentified compounds (yellow to orange, presumably phosphine-substituted products of decomposed starting cluster) and a broad dark red band of **5** (110 mg, 45%). Single crystals of this cluster suitable for an X-ray diffraction study were obtained by recrystallization from a hexane/octane mixture at -15 °C. IR (hexane; ν(CO)/cm<sup>-1</sup>): 2065 s, 2036 vs, 2001 s, 1991 m, 1964 m, 1936 w, 1927 vw, 1790 m. MS ES (*m/z*): [M<sup>+</sup>] 1331 (calcd 1330). <sup>31</sup>P{<sup>1</sup>H} NMR (CDCl<sub>3</sub>, 25 °C; δ): 90.4 (unresolved multiplet). <sup>1</sup>H NMR (toluene-*d*<sub>6</sub>, 25 °C; δ): 7.37 (t, pyrrole, 1H, *J*(H–H) = 3.7 Hz), 7.22 (m, Ph, 1H), 7.20 (m, Ph, 1H), 7.14–7.07 (m, Ph, 5H), 7.06 (m, pyrrol, 1H), 6.85–6.76 (m, Ph, 5H), 6.79 (m, thienyl, 1H), 6.47 (dd, thienyl, 1H, *J*(H–H) = 6.9, 3.4 Hz), 6.20 (dd, thienyl, 1H, *J*(H–H) = 4.9, 4.0 Hz), 5.92 (d, pyrrole, 1H, *J*(H–H) = 4.1 Hz), 5.60 (s, Cp, 5H), 5.55 (d, pyrrole, 1H, *J*(H–H) = 3.4 Hz), 4.82 (dd, oxazoline CH, 1H, *J*(H–H) = 9.6, 8.2 Hz), 4.25–4.18 (m, oxazoline CH<sub>2</sub>, 2H), 4.02–3.96 (m, oxazoline CH<sub>2</sub>, 2H), 3.80 (dd, oxazoline CH, 1H, *J*(H–H) = 8.2, 4.1 Hz), 2.28 (m, *i*-Pr CH, 1H, *J*(H–H) = 6.9, 2.7 Hz), 1.63 (m, *i*-Pr CH, 1H, *J*(H–H) = 6.9 Hz), 1.10 (d, *i*-Pr CH<sub>3</sub>, 3H, *J*(H–H) = 6.9 Hz), 0.79 (d, *i*-Pr CH<sub>3</sub>, 3H, *J*(H–H) = 6.9 Hz), 0.57 (d, *i*-Pr CH<sub>3</sub>, 3H, *J*(H–H) = 7.6 Hz), -0.12 (d, *i*-Pr CH<sub>3</sub>, 3H, *J*(H–H) = 6.9 Hz), -15.82 (dd, 1H, *J*(H–P) = 11.7 Hz, *J*(H–H) = 2.1 Hz), -20.55 (dd, 1H, *J*(H–P) = 8.9 Hz, *J*(H–H) = 2.1 Hz). Anal. Calcd for C<sub>50</sub>H<sub>44</sub>N<sub>4</sub>O<sub>10</sub>PSRhRu<sub>3</sub>·C<sub>8</sub>H<sub>18</sub>: C, 48.23; H, 4.33; N, 3.88. Found: C, 48.30; H, 4.44; N, 3.88.

**X-ray Structure Determinations.** The data for **4** and **5** were collected on a Nonius Kappa-CCD diffractometer using monochromated Mo Kα radiation. Each data set was measured using a combination of φ scans and ω scans with κ offsets, to fill the Ewald sphere. The data were processed using the Denzo-SMN package.<sup>16</sup> Absorption corrections were carried out using SORTAV.<sup>17</sup> The structure was solved and refined using SHELXTL version 6.1<sup>18</sup> for full-matrix least-squares refinement that was based on *F*<sup>2</sup>. The positions of the hydride atoms were located from a difference Fourier map. During the refinement, all of the Ru–H distances were constrained to be 1.67(1) Å. The thermal parameters of the hydrides were tied to the atoms Ru1A and Ru1B so that *U*<sub>eq</sub>(H) = 1.3[*U*<sub>eq</sub>(Ru)]. Crystallographic data for compounds **4** and **5** are given in Table 1.

(16) Otwinowski, Z.; Minor, W. 1997. *Macromolecular Crystallography*; Methods in Enzymology 276; Carter, C. W., Sweet, R. M., Eds.; Academic Press: London, 1997; Part A, pp 307–326.

(17) Blessing, R. H. *Acta Crystallogr.* **1995**, *A51*, 33.

(18) Sheldrick, G. M. SHELXTL version 6.1; Bruker AXS, Madison, WI, 2001.



**Table 1. Crystal Data and Structure Refinement for 4 and 5**

	4	5
empirical formula	C <sub>39</sub> H <sub>41</sub> Cl <sub>5</sub> N <sub>4</sub> O <sub>2</sub> PRhS	C <sub>53</sub> H <sub>51</sub> N <sub>4</sub> O <sub>10</sub> PRhRu <sub>3</sub> S
formula wt	940.95	1373.13
temp, K	150(1)	150(1)
wavelength, Å	0.710 73	0.710 73
cryst syst	monoclinic	monoclinic
space group	<i>P</i> 2 <sub>1</sub>	<i>P</i> 2 <sub>1</sub>
unit cell dimens		
<i>a</i> , Å	13.0617(2)	13.0819(4)
<i>b</i> , Å	11.3621(2)	37.6066(10)
<i>c</i> , Å	13.6659(2)	13.1271(3)
α, deg	90	90
β, deg	90.5678(12)	110.0017(12)
γ, deg	90	90
<i>V</i> , Å <sup>3</sup>	6817.0(3)	6068.5(3)
<i>Z</i>	2	4
calcd density, Mg/m <sup>3</sup>	1.541	1.503
abs coeff, mm <sup>-1</sup>	0.882	1.114
goodness of fit on <i>F</i> <sup>2</sup>	1.050	0.992
final <i>R</i> indices	R1 = 0.0307,	R1 = 0.0558,
( <i>I</i> > 2σ( <i>I</i> ))	wR2 = 0.0673	wR2 = 0.1199
<i>R</i> indices (all data)	R1 = 0.0354,	R1 = 0.0944,
	wR2 = 0.0704	wR2 = 0.1341

## Results and Discussion

**The (S,S)-BOTPHOS Ligand.** The reaction sequence presented in Scheme 1 affords a chiral bis(oxazoline) phosphine ((S,S)-BOTPHOS, **3**) in a total yield close to 25%, which is rather good for a three-stage synthesis. The ligand contains four potentially coordinating donor centers: two oxazoline nitrogens, the phosphorus atom, and the sulfur in the thienyl phosphorus substituent. This gives substantial flexibility to the ligand in its coordination modes, especially in polynuclear cluster complexes. The composition and structure of the ligand shown in Scheme 1 were established by elemental analysis, mass spectroscopic data and <sup>1</sup>H NMR studies, and the structure of **3** was later confirmed by the crystallographic analysis of the complexes formed in reactions of **3** with binuclear and tetranuclear transition-metal complexes (Table 2, Figures 1 and 3). The presence of two chiral structural units located in the oxazoline rings was verified by the CD spectrum, which displays clear Cotton responses in the 200–320 nm range, as shown in Figure S1.<sup>47</sup> The well-known chemistry involved in the formation of oxazoline rings<sup>2</sup> allows the assignment of the *S* configuration to the chiral carbon atoms because of the use of L-valinol in the synthesis. The ligand backbone consists of three condensed rings (one phosphadiazole and two pyrrole systems) that makes it exceptionally rigid in a way similar to that in pybox type tridentate (N,N,N) ligands such as 2,6-bis(4,4-dimethyloxazolin-2-yl)pyridine.<sup>4</sup> However, in contrast to the N,N,N ligands,<sup>4</sup> the structure of **3** belongs to a non-*C*<sub>2</sub>-symmetric group that may, in principle, enhance the performance of catalysts containing this ligand. This assumption has been theoretically analyzed<sup>19</sup> and experimentally supported<sup>20</sup> in recent publications.

**The Complex RhCl<sub>2</sub>(CH<sub>2</sub>Cl)((S,S)-BOTPHOS) (4).** The reaction of (S,S)-BOTPHOS with the binuclear

rhodium carbonyl chloride in dichloromethane, Rh<sub>2</sub>(CO)<sub>4</sub>-Cl<sub>2</sub>, affords the mononuclear Rh(III) complex RhCl<sub>2</sub>-(CH<sub>2</sub>Cl)((S,S)-BOTPHOS) (**4**). This complex easily gave single crystals suitable for an X-ray analysis, and its solid-state structure has been established crystallographically. The crystallographic data and selected structural parameters are given in Tables 1 and 2, respectively, and its molecular structure is shown in Figure 1.

The molecule consists of a six-coordinated Rh(III) ion bound to two chlorides, a CH<sub>2</sub>Cl moiety, and the (S,S)-BOTPHOS ligand. The latter is coordinated to the metal center through the phosphorus and two oxazoline nitrogen atoms in the so-called N,P,N manner. The oxidation of Rh(I) to Rh(III) in the course of the reaction is evidently a result of the oxidative addition of a dichloromethane solvent molecule to the intermediate Rh(I) complex, as confirmed by the presence of the chloromethyl radical in the coordination sphere of **4**. A similar oxidative addition of dichloromethane and other chlorinated organic compounds to a Rh(I) complex in the presence of an N,N,N type, dm-pybox ligand was observed earlier.<sup>21</sup> On the basis of the NMR spectroscopic data, the authors ascribed to their products structures completely analogous to that found for **4**. The phosphorus and two nitrogen atoms of coordinated BOTPHOS in **4** form a *mer* structural pattern, as in the case of the tridentate nitrogen ligand mentioned above.<sup>4</sup> The chloromethyl radical occupies a *cis* position with respect to all BOTPHOS coordinating centers. One of the chlorides occupies another *cis* position relative to BOTPHOS, being *trans* to the chloromethyl ligand. The second chloride takes up the position *trans* to the phosphorus site to complete the octahedral arrangement of the rhodium ion. It has to be noted that the *mer* coordination mode of the tridentate (N,N,N) bis(oxazoline)pyridine ligands is quite typical for Rh<sup>4,22–24</sup> and Ru<sup>25–28</sup> octahedral complexes, due evidently to the ligands' rigid backbones, where three nitrogen donor atoms are nearly coplanar with the pyridine ring plane. The more flexible backbones of the N,P,N bis(oxazoline) phosphines and bis(oxazoline) phosphonites (which contain –CH<sub>2</sub>– and –OC(Me)<sub>2</sub>– groups, respectively, between the phosphorus atoms and oxazoline rings) allow both *mer*<sup>6,29</sup> and *fac*<sup>6,30</sup> coordination of the tridentate ligands in ruthenium and palladium complexes.<sup>2</sup> It seems that the BOTPHOS ligand is closer in its geometry to the pybox (N,N,N) ligand series<sup>2,4,21</sup> because of the rigid backbone of condensed phosphadiazole and pyrrole rings.

(21) Nishiyama, H.; Horihata, M.; Hirai, T.; Wakamatsu, S.; Itoh, K. *Organometallics* **1991**, *10*, 2706.

(22) Nishiyama, H.; Niwa, E.; Inoue, T.; Ishima, Y.; Aoki, K. *Organometallics* **2002**, *21*, 2572.

(23) Nishiyama, H.; Hirai, T.; Itoh, K. *J. Organomet. Chem.* **1992**, *431*, 227.

(24) Cuervo, D.; Diez, J.; Gamasa, M. P.; Garcia-Granda, S.; Gimeno, J. *Inorg. Chem.* **2002**, *41*, 4999.

(25) Cadierno, V.; Gamasa, M. P.; Gimeno, J.; Iglesias, L.; Garcia-Granda, S. *Inorg. Chem.* **1999**, *38*, 2874.

(26) Hua, X.; Shang, M.; Lappin, A. G. *Inorg. Chem.* **1997**, *36*, 3735.

(27) Shiotsuki, M.; Suzuki, T.; Iida, K.; Ura, Y.; Wada, K.; Kondo, T.; Mitsudo, T. *Organometallics* **2003**, *22*, 1332.

(28) Motoyama, Y.; Kurihara, O.; Murata, K.; Aoki, K.; Nishiyama, H. *Organometallics* **2000**, *19*, 1025.

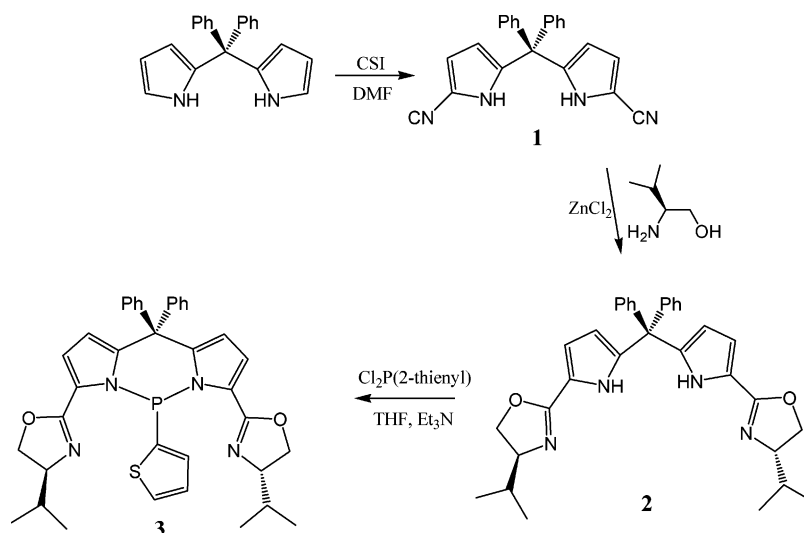
(29) Braunstein, P.; Naud, F.; Dedieu, A.; Rohmer, M.-M.; DeCian, A.; Rettig, S. J. *Organometallics* **2001**, *20*, 2966.

(30) Braunstein, P.; Fryzuk, M. D.; Naud, F.; Rettig, S. J. *J. Chem. Soc., Dalton Trans.* **1999**, 589.

(19) Gleich, D.; Herrmann, W. A. *Organometallics* **1999**, *18*, 4354.

(20) Reetz, M. T.; Gosberg, A. *Tetrahedron: Asymmetry* **1999**, *10*, 2129.

## Scheme 1



The bond length parameters in **4** (Table 2) do not display substantial distortions compared to similar oxazoline-containing complexes of transition metals. The rhodium to oxazoline nitrogen bond lengths, 2.077(3) and 2.073(3) Å, fall in the range typical for analogous *mer*-N,P,N<sup>6,29</sup> and N,N,N<sup>4,22</sup> complexes. The rhodium to phosphorus bond length of 2.1612(8) Å does not deviate from the bond distances found in other phosphine complexes of this type.<sup>6,29</sup> The bond lengths in the coordinated oxazoline rings are also very close to the values found for these organic moieties in related transition-metal complexes.<sup>6,29,30</sup>

The oxazoline rings in **4** form essentially nonplanar systems, due to the sp<sup>3</sup> hybridization of both CH<sub>2</sub> and C(H)(*i*-Pr) carbon atoms. Nevertheless, the C(7)N(1)-C(5)O(1) and C(13)N(2)-C(11)O(2) fragments of these rings are nearly planar, the corresponding torsion angles being 5.7 and 3.9°. All but two of the octahedral angles are close to the normal value of 90°. The Cl(1) ligand is bent away from the N(1)C(5)O(1)C(6)C(7) oxazoline ring, due to an interaction with one of the *i*-Pr substituents to form the Cl(1)-Rh(1)-N(1) angle of 97.5°. Another clearly visible angular distortion is the C(17)-Rh(1)-P(1) angle of 96.6°, which is evidently dictated by intramolecular interactions between the ligands around the rhodium center. It is worth noting that these interactions are not of a purely van der Waals nature, because short contacts between the chloride ions and organic protons inevitably have an attractive component, which stabilizes the structure and strengthens the molecular conformation in both the solid and liquid states. Of these contacts, it is necessary to highlight the Cl(2)-H(17a), Cl(2)-H(14a), and Cl(1)-H(8a) distances, which are 2.734, 2.546, and 2.632 Å, respectively. These figures are definitely smaller than the sum of van der Waals radii for these elements (2.97 Å<sup>31</sup>), and clearly point to the presence of hydrogen bonding between these pairs of atoms. The corresponding hydrogens belong to a coordinated chloromethyl fragment and one of the *i*-Pr substituents of oxazolines, and these hydrogen bonds evidently play an important role in the structural configuration of **4**. As is discussed below, they also affect the VT properties of the proton

spectra, making the molecular configuration in solution unusually rigid over a wide temperature range.

The NMR spectroscopic data (1D <sup>1</sup>H (Figure 2), <sup>1</sup>H COSY (Figure S2),<sup>47</sup> <sup>1</sup>H-<sup>13</sup>C HSQC (Figure S3)<sup>47</sup>) obtained for **4** clearly show that the structure found in the solid state remains unchanged in solution. The combination of 1D and 2D NMR routines allows complete assignment of the <sup>1</sup>H spectrum, as shown in the upper part of Figure 2.

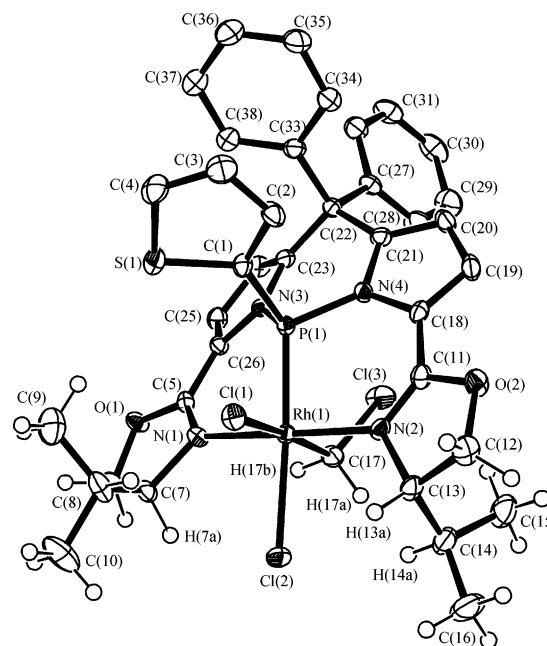
In the room-temperature <sup>1</sup>H spectrum all protons, including those of the CH<sub>2</sub>Cl ligand and the CH protons of *i*-Pr, thienyl, and phenyl radicals, appear as clearly resolved signals that are indicative of an absolutely rigid molecular conformation under these conditions. Rotation of the CH<sub>3</sub> groups about HC-CH<sub>3</sub> bonds is the only dynamic process detectable on the NMR time scale at room temperature. This striking observation clearly points to the presence of important intramolecular interactions, which dictate the fine details of the molecular configuration. The chloride to proton hydrogen bonding mentioned above seems to be of particular importance for the stereochemical rigidity of the CH<sub>2</sub>Cl ligand. In fact, the protons of this group are diastereotopic and one might expect (even in the case of fast rotation about the Rh-C bond) the appearance of the proton signals as an AB system. However, the signals emerge in the spectrum as clearly resolved dd resonances (*J*(H-H) = 5.9 Hz, *J*(Rh-H) = 3.2 and 2.7 Hz) separated by ca. 1 ppm (see Figure 2). This difference is very likely indicative of the interaction of a proton with the Cl(2) ligand. Again, the CH<sub>3</sub> groups of the *i*-Pr radicals are diastereotopic, both in the free ligand and in this rhodium complex, and should give rise to four independent resonances in the proton spectrum of **3** and **4**. However, the methyl resonances in the spectrum of the free ligand are not completely resolved (1.04, 0.61 ppm), whereas in the spectrum of **4** one can observe four well-separated (0.96, 0.83, 0.78, 0.63 ppm) methyl group signals. This very probably suggests restricted rotation of the *i*-Pr radicals in **4**. The signals do not display significant chemical shift differences compared to the free ligands. In contrast, the signals of CH(*i*-Pr) protons in **4** are shifted substantially downfield (3.41, 3.28 ppm) compared to the corresponding resonances (1.73, 1.48

(31) Bondi, J. J. *Phys. Chem.* **1964**, *68*, 441.

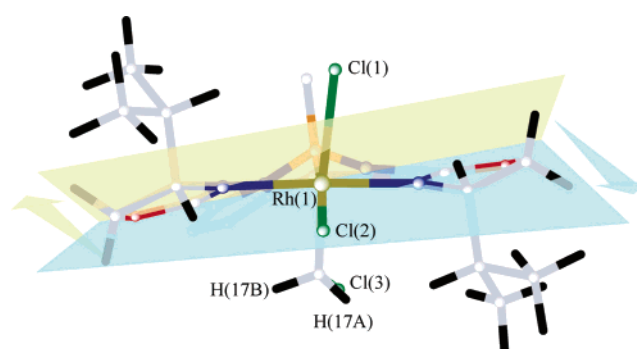
**Table 2. Selected Bond Lengths (Å) and Angles (deg) for 4 and 5**

Bond Lengths			
Compound 4			
Rh(1)–N(1)	2.077(3)	Rh(1)–P(1)	2.1612(8)
Rh(1)–N(2)	2.073(3)	Rh(1)–Cl(1)	2.4747(7)
Rh(1)–C(17)	2.075(3)	Rh(1)–Cl(2)	2.4277(8)
P(1)–C(1)	1.769(3)	P(1)–N(4)	1.686(2)
P(1)–N(3)	1.698(3)		
C(17)–Cl(3)	1.796(3)		
N(1)–C(5)	1.292(4)	O(1)–C(6)	1.467(4)
N(1)–C(7)	1.497(4)	O(1)–C(5)	1.345(4)
C(6)–C(7)	1.524(5)		
N(2)–C(11)	1.292(4)	O(2)–C(12)	1.469(4)
N(2)–C(13)	1.487(4)	O(2)–C(11)	1.344(4)
C(12)–C(13)	1.527(5)		
Compound 5			
Rh(1A)–Ru(1A)	2.7487(10)	Ru(1A)–Ru(2A)	2.8551(10)
Rh(1A)–Ru(2A)	2.6740(10)	Ru(1A)–Ru(3A)	2.9498(10)
Rh(1A)–Ru(3A)	2.7671(11)	Ru(2A)–Ru(3A)	2.7643(10)
Ru(1A)–C(1A)	1.852(10)	Ru(3A)–C(7A)	1.878(10)
Ru(2A)–C(3A)	1.870(10)	Ru(3A)–C(8A)	1.893(11)
Ru(2A)–C(4A)	1.923(11)	Rh(1A)–C(2A)	1.899(11)
Ru(2A)–C(5A)	1.904(9)	Ru(3A)–C(2A)	2.234(10)
Ru(3A)–C(6A)	1.860(11)		
Ru(1A)–P(1A)	2.234(2)	Ru(1A)–N(1A)	2.145(7)
Ru(1A)–H(1)	1.671(10)	Ru(1A)–H(2)	1.676(10)
Ru(2A)–H(1)	1.671(10)	Ru(3A)–H(2)	1.673(10)
P(1A)–N(2A)	1.755(7)	P(1A)–C(14A)	1.800(8)
P(1A)–N(3A)	1.753(7)		
N(1A)–C(18A)	1.288(11)	O(9A)–C(18A)	1.381(10)
N(1A)–C(19A)	1.499(11)	O(9A)–C(20A)	1.504(11)
C(19A)–C(20A)	1.530(13)	C(18A)–C(24A)	1.430(13)
N(4A)–C(33A)	1.246(10)	O(10A)–C(34A)	1.417(11)
N(4A)–C(35A)	1.490(15)	O(10A)–C(33A)	1.371(10)
C(34A)–C(35A)	1.569(16)	C(32A)–C(33A)	1.427(12)
Bond Angles			
Compound 4			
P(1)–Rh(1)–Cl(1)	88.94(3)	N(2)–Rh(1)–C(17)	90.87(11)
P(1)–Rh(1)–C(17)	96.64(9)	N(2)–Rh(1)–Cl(2)	93.17(7)
N(1)–Rh(1)–P(1)	87.96(7)	N(2)–Rh(1)–Cl(1)	85.17(7)
N(1)–Rh(1)–Cl(1)	97.52(7)	C(17)–Rh(1)–N(1)	86.58(11)
N(1)–Rh(1)–Cl(2)	88.11(7)	C(17)–Rh(1)–Cl(2)	83.33(9)
N(2)–Rh(1)–P(1)	90.76(7)	Cl(2)–Rh(1)–Cl(1)	91.37(3)
Compound 5			
C(1A)–Ru(1A)–N(1A)	96.1(3)	N(1A)–Ru(1A)–Ru(3A)	100.0(2)
C(1A)–Ru(1A)–P(1A)	101.4(3)	P(1A)–Ru(1A)–Ru(3A)	109.31(7)
C(1A)–Ru(1A)–Rh(1A)	90.9(3)	P(1A)–Ru(1A)–Ru(2A)	117.47(7)
C(1A)–Ru(1A)–Ru(2A)	96.6(3)	Rh(1A)–Ru(1A)–Ru(2A)	56.96(2)
N(1A)–Ru(1A)–P(1A)	85.7(2)	Rh(1A)–Ru(1A)–Ru(3A)	57.97(3)
N(1A)–Ru(1A)–Rh(1A)	96.5(2)	Ru(2A)–Ru(1A)–Ru(3A)	56.85(2)

ppm) of the free ligand. These differences may occur as a result of the interaction of both protons with the chloride ions, which may also hinder free rotation of the *i*-Pr radicals. Conformational rigidity of both phenyl rings and the thienyl substituent is very likely a consequence of the interaction of the Cl(3) atom with the hydrogen attached to the C(28) atom (shown by the 3.13 Å Cl–H distance) and of the stacking of the adjacent phenyl and thienyl rings, which are nearly coplanar in the solid-state structure. Variable-temperature NMR experiments in *d*<sub>6</sub>-benzene (Figure S4)<sup>47</sup> showed that **4** keeps its rigidity between 25 and 65 °C. In this temperature range neither the *i*-Pr groups nor the phenyl rings rotate about the single C–C bonds. It is not surprising that we also do not observe any conformational flexibility arising from a symmetry exchange between oxazoline rings or between pyrrole rings of the ligand backbone.

**Figure 1.** ORTEP plot of the molecular structure of RhCl<sub>2</sub>(CH<sub>2</sub>Cl)((*S,S*)-BOTPHOS) (**4**). Thermal ellipsoids are drawn at the 30% level.

From the viewpoint of stereochemistry, the rigid tridentate coordination of (*S,S*)-BOTPHOS to the rhodium ion introduces a new chiral element in the molecule. The planar C–N–C–O fragments of the oxazoline rings are twisted relative to each other so as to give a dihedral angle of 7.25(1)° between the averaged centroids of C(7),N(1),C(5),O(1) and C(13),N(2),C(11),O, and as indicated in Chart 1, this leads to a helical structure in an *S* conformation.

**Chart 1**

The rigidity of the molecular conformation is supported by the intramolecular hydrogen bonding mentioned above and by the steric hindrance between two *i*-Pr radicals which would accompany any reorientation of the oxazoline rings. The stereochemistry of this structural pattern looks very similar to the atropoisomerism of biaryl- and binaphthyl-substituted moieties which is well-known in coordination chemistry. It is very likely that appearance of this new stereogenic center, which incorporates the metal atom and the corresponding *d* orbitals, results in extension of the CD spectroscopic response into the longer wavelength area compared to the free BOTPHOS ligand. The CD spectrum of **4** (Figure S5)<sup>47</sup> shows relatively strong absorption up





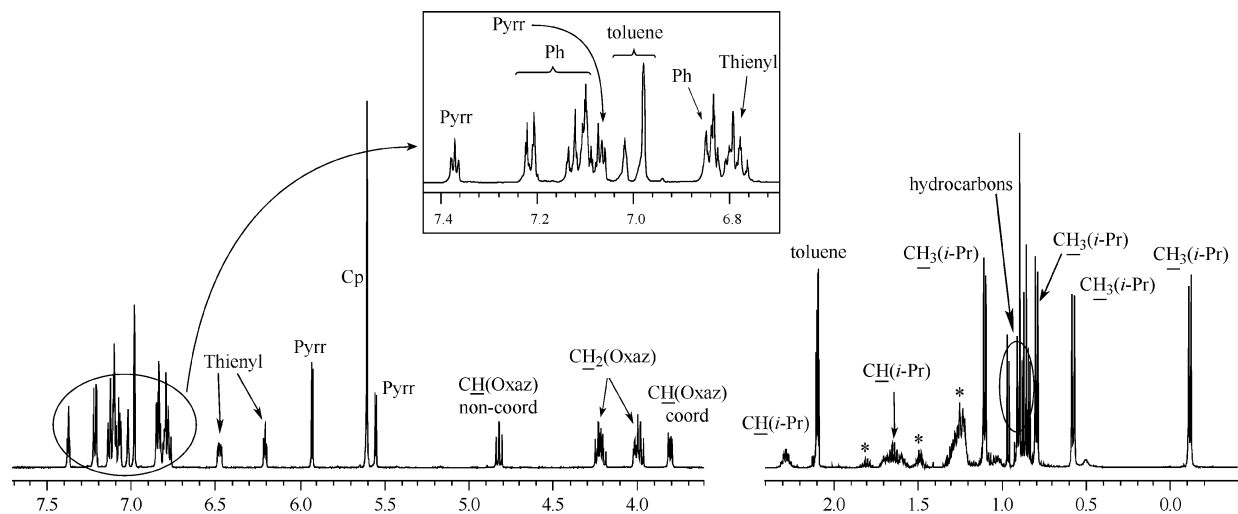
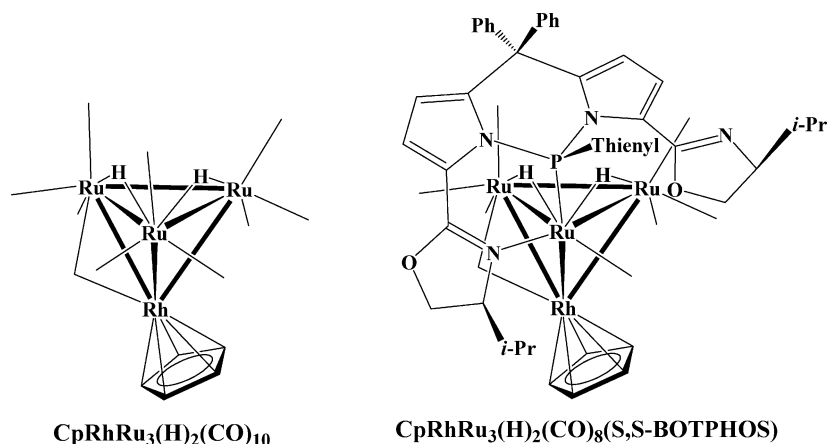


**Figure 4.** 500 MHz  $^1\text{H}$  NMR spectrum of **5** in the organic region ( $d_8$ -toluene, 25 °C). The inset shows the expanded aromatic area of the spectrum.

**Chart 2**



through the phosphorus and thienyl sulfur,<sup>38</sup> and  $\mu_3$  coordination through the phosphorus and a metalated thienyl ring in a  $\sigma$ - $\pi$  vinyl coordination mode.<sup>39</sup> Neither of these opportunities has been realized in the present case, very probably due to the substantial steric demands of the BOTPHOS ligand and rigidity of its backbone.

The substitution of two COs does not change the positions of the remaining eight carbonyl ligands, one of which occupies a semibringing position on the Ru(3A)-Rh(1A) edge as in the parent cluster.<sup>37</sup> The semibringing carbonyl is substantially shifted to the rhodium atom (see Table 2), as it is in the unsubstituted precursor. The Rh-Ru bond lengths in the tetrahedron do not differ considerably, falling in the range 2.6740–2.7671 Å, which is very similar to those in the unsubstituted cluster.<sup>37</sup> The three Ru-Ru distances in **5** are strongly differentiated, depending on whether they are bridged by a hydride ligand or not. The nonbridged Ru(2)-Ru(3) bond (2.7643 Å) is substantially shorter compared to the hydride-bridged Ru(1)-Ru(2) and Ru(1)-Ru(3) edges (2.8551 and 2.9498 Å, respectively). This observation is completely consistent with the bond

lengthening effect of the hydrides<sup>40–42</sup> in both **5** and the parent  $\text{CpRhRu}_3(\text{H})_2(\text{CO})_{10}$  cluster.<sup>37</sup> The hydride ligands were located using a difference Fourier map, and their positions on the Ru(1)-Ru(2) and Ru(1)-Ru(3) edges were confirmed by analysis of the  $^1\text{H}$  spectrum in the hydride area. Comparison of the bond lengths in coordinated and noncoordinated oxazoline rings shows the expected elongation of the “double” C=N bond upon coordination from 1.246(10) to 1.288(11) Å. Another effect of the bonding of the oxazoline moiety to the Ru(1) atom consists of lengthening of the O(9A)-C(20A) bond to 1.504(11) Å, compared with the 1.417(11) Å for the analogous O(10A)-C(34A) distance in the noncoordinated oxazoline ring.

The IR and  $^1\text{H}$  NMR spectroscopic data obtained for **5** in solution are consistent with the structure of this cluster, found in the solid state. The IR spectrum in the carbonyl area displays strong absorption bands corresponding to terminal COs (2100–1900  $\text{cm}^{-1}$ ) together with a band at 1790  $\text{cm}^{-1}$ , which can be assigned to the bridging carbonyl ligand. The 1D  $^1\text{H}$  (Figure 4) and  $^1\text{H}$

(38) Tunik, S. P.; Koshevoy, I. O.; Poë, A. J.; Farrar, D. H.; Nordlander, E.; Haukka, M.; Pakkanen, T. A. *Dalton* **2003**, 2457.

(39) Deeming, A. J.; Jayasuriya, S. N.; Arce, A. J.; DeSanctis, Y. *Organometallics* **1996**, 15, 786.

(40) Bruce, M. I.; Horn, E.; Bin Shawkataly, O.; Snow, M. R.; Tiekink, E. R. T.; Williams, M. L. *J. Organomet. Chem.* **1986**, 316, 187.

(41) Churchill, M. A.; Lashewicz, R. A.; Shapley, J. R.; Richter, S. I. *Inorg. Chem.* **1980**, 19, 1277.

(42) Homanen, P.; Persson, R.; Haukka, M.; Pakkanen, T. A.; Nordlander, E. *Organometallics* **2000**, 19, 5568.



COSY (Figure S6)<sup>47</sup> spectra of **5** in the “organic” region are clearly resolved and allow the unambiguous assignment of the signals, as shown in the upper part of Figure 4.

As in the case of **4**, the room-temperature spectrum is consistent with the rigid structure of the ligand backbone and chiral oxazoline substituents. The <sup>1</sup>H spectrum in the hydride area exhibits two dd resonances corresponding to nonequivalent hydrides. Their positions (−15.82 and −20.55 ppm) are indicative of the bridging coordination mode of both ligands. The large spin–spin coupling constants have been assigned to the <sup>31</sup>P–<sup>1</sup>H interaction on the basis of a <sup>31</sup>P decoupling experiment (Figure S7).<sup>47</sup> The small coupling constant originates from the hydride coupling and fits well with the values found earlier in the phosphine-substituted tetranuclear ruthenium hydride clusters.<sup>43</sup> To study the dynamic behavior of **5** in solution, the variable-temperature <sup>1</sup>H experiments were performed in *d*<sub>8</sub>-toluene in the temperature range 25–85 °C. The chelate bidentate coordination of BOTPHOS in **5** implies a possibility of exchange dynamics involving oxazoline arms, similar to that observed in mononuclear Pd(II) complexes.<sup>2,29</sup> The VT NMR study of the palladium allyl complex containing the bis(oxazoline) phosphonito ligand<sup>29</sup> showed that this is a very low barrier process, which averaged the signals of the coordinated and free oxazoline moieties at about 205 K. In contrast to this, we did not observe broadening of the resonances corresponding to bonded and nonbonded oxazoline fragments in the <sup>1</sup>H spectra of **5** up to 85 °C (Figure S8).<sup>47</sup> This is indicative of much stronger bonding of the oxazoline nitrogen to Ru(0) compared to Pd(II).

The stereochemistry of **5** is another example of very highly diastereoselective reactions of chiral bidentate ligands with tetranuclear clusters. The molecular structure of **5** displays an interesting example of how the ligand coordination may give rise to a few other stereogenic centers. In addition to the two *S*-chiral centers in BOTPHOS, the structure of **5** contains a chiral phosphorus atom in a tetrahedral environment with four different substituents. The *S* arrangement of the *i*-Pr radicals in the oxazoline rings evidently dictates the phosphorus atom chirality to give its *S* stereoconfiguration. This type of asymmetry, generated by selective ligation of a potentially tridentate phosphine to a metal center in a bidentate manner, was also observed in a Pd(II) complex containing (NPN) bis(oxazoline) phosphine.<sup>7</sup> Similarly to what occurs in **5**, the (*S,S*)-bis(oxazoline) phosphine coordinates to the palladium ion in the  $\kappa^2$  mode to give an *S* configuration of the phosphorus stereogenic center. It has to be noted that this reaction displays quantitative distereoselectivity (de), in that the X-ray and NMR spectroscopic studies of the complexes obtained clearly demonstrate that only one *S,S,S,S* diastereomer is present in the isolated products, both in the solid state and in solution.

The cluster structure of **5** also gives rise to an additional stereogenic center in this molecule. The “RhRu<sub>3</sub>” cluster framework is asymmetric too, because the ligand environments of all three ruthenium atoms are different. Considering the metal tetrahedron as an

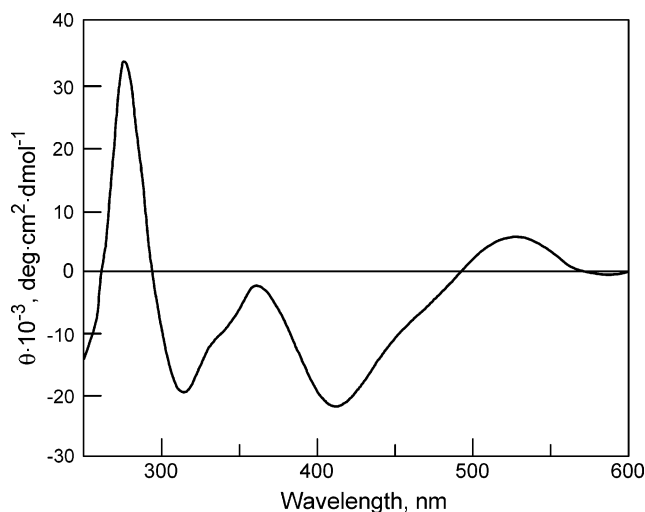


**Figure 5.** Circular dichroism spectrum of **5** (hexane, 20 °C).

analogue of an asymmetric carbon atom, one can ascribe the *S* configuration to the “RhRu<sub>3</sub>” framework on the basis of CIP rules,<sup>44</sup> to give the *S,S,S,S* configuration to the molecule as a whole. Refinement of the crystal structure of **5** in the *P2*<sub>1</sub> space group implies that only one stereoconfiguration is present in the crystal studied. Analysis of the NMR spectroscopic properties of the bulk sample also points to the existence of only one diastereomer in solution, and the stereochemical rigidity of **5** indicates that the molecular configuration remains unchanged over a wide temperature range. The CD spectrum of **5** (Figure 5) shows that Cotton responses continue up to 600 nm. In cluster complexes the lowest energy absorption bands (400–600 nm for **5**) are normally assigned to the transitions between bonding and antibonding orbitals of the metal skeleton<sup>32</sup> (see also ref 45). Appearance of the CD signals in this area is consistent with the asymmetry of the cluster core and can be considered as further proof of quantitative diastereoselection in the reaction under investigation.

All these observations clearly point to 100% de in formation of the specific stereoconfiguration of **5** under control of the BOTPHOS ligand. This is not a common case in cluster chemistry, and as a rule the isolation of a pure diastereomer (“cluster framework–ligand” chiral centers) needs additional separation procedures. For example, HPLC purification<sup>46</sup> had to be applied to obtain the diastereomers of triosmium clusters containing chiral moieties in metalated (*S*)-nicotine and (*R*)-1-(4-pyridyl)ethanol ligands. It is worth noting that recently<sup>43</sup> another example of this sort was reported, where 100% de was observed in the reaction of *S*-BINAP with H<sub>4</sub>Ru<sub>4</sub>(CO)<sub>12</sub>. This reaction also gave only one stereoconfiguration of the tetranuclear cluster framework, in which all ruthenium atoms were different due to the difference in their ligand environment. These results mean that a proper choice of inductive chiral

(44) *Pure Appl. Chem.* **1976**, *45*, 11.

(45) Sizova, O. V.; Baranovskii, V. I. *Inorg. Chim. Acta* **1993**, *214*, 113.

(46) Deeming, A. J.; Stchedroff, M. J.; Whittaker, C.; Arce, A. J.; De Sanctis, Y.; Steed, J. W. *J. Chem. Soc., Dalton Trans.* **1999**, 3289.

(47) Some of the spectroscopic data obtained are available as Supporting Information, and the numbers of the corresponding figures bear the “S” prefix.

(43) Tunik, S. P.; Pilyugina, T. S.; Koshevoy, I. O.; Selivanov, S. I.; Haukka, M.; Pakkanen, T. A. *Organometallics* **2004**, *23*, 568.

ligand may provide unusually high de in reactions of cluster complexes, and these reactivity patterns may form a background for application of the cluster compounds in asymmetric catalysis, which is still a nearly unexplored area.

**Acknowledgment.** Financial support provided by the Nordic Council of Ministers (I.O.K., S.P.T.), the Natural Science and Engineering Research Council of Canada, the Russian Foundation for Basic Research (Grant No. 02-03-32792), and NATO (for a postdoctoral

fellowship to I.O.K.) is gratefully acknowledged. We also wish to thank Ms. Päivi Joensuu (University of Oulu) for the mass spectroscopic measurements.

**Supporting Information Available:** Tables and figures giving crystallographic data, CD spectra, and  $^1\text{H}$  VT,  $^1\text{H}$  COSY, and  $^1\text{H}$ - $^{13}\text{C}$  HSQC NMR spectra; crystallographic data are also available as CIF files. This material is available free of charge via the Internet at <http://pubs.acs.org>.

OM0498450